Journal of Microbiology (2022) Vol. 60
DOI 10.1007/s12275-022-2250-5
eISSN 1976-3794
pISSN 1225-8873

Description of *Deefgea piscis* sp. nov., and *Deefgea tanakiae* sp. nov., isolated from the gut of Korean indigenous fish[§]

Do-Hun Gim[1†], So-Yeon Lee[1†], Jeong Eun Han[1†], Jae-Yun Lee[2], Seo Min Kang[1], and Jin-Woo Bae[1,2*]

[1]*Department of Biology and Department of Biomedical and Pharmaceutical Sciences, Kyung Hee University, Seoul 02447, Republic of Korea*
[2]*Department of Life and Nanopharmaceutical Sciences and Department of Biology, Kyung Hee University, Seoul 02447, Republic of Korea*

(Received Jun 7, 2022 / Revised Aug 4, 2022 / Accepted Aug 9, 2022)

Three novel strains, (D17^T, D13, and D25^T) isolated from the gut of the Korean dark sleeper (*Odontobutis platycephala*), Kumgang fat minnow (*Rhynchocypris kumgangensis*), and the Korean oily bitterling (*Tanakia koreensis*) were identified as two novel species. Strains D17^T and D13 showed the highest similarities in 16S rRNA gene and complete genome sequences to *Deefgea rivuli* WB 3.4-79^T (98.0% and 97.9%, respectively, of 16S rRNA gene sequence similarity, 77.8% and 77.7%, respectively, of orthologous average nucleotide identity, OrthoANI, and 21.9% and 21.9%, respectively, of digital DNA-DNA hybridization, dDDH). Strain D17^T showed the highest similarities in 16S rRNA gene and complete genome sequences to D13 (99.9% of 16S rRNA gene sequence similarity, 91.8% of OrthoANI, and 45.1% of dDDH); therefore, strains D17^T and D13 were assigned as the same species. Strain D25^T showed the highest similarities in 16S rRNA gene and complete genome sequences to *D. chitinilytica* Nsw-4^T (98.2% of 16S rRNA gene sequence similarity, 82.4% of OrthoANI, and 25.1% of dDDH). Strains D17^T and D13 were Gram-stain-negative, facultative anaerobes, rod-shaped, non-motile, and non-flagellated. Strain D25^T was Gram-stain-negative, facultative anaerobe, rod-shaped, and motile by a single polar flagellum. These strains had $C_{16:0}$ and summed feature 3 ($C_{16:1}$ *ω7c* and/or $C_{16:1}$ *ω6c*) as the major cellular fatty acids and possessed Q-8 as a major respiratory ubiquinone. All three strains contained phosphatidylethanolamine and phosphatidylglycerol as the major polar lipids. Based on polyphasic taxonomic data, strains D17^T, D13, and D25^T represent two novel species of the genus *Deefgea*. We propose the name *Deefgea piscis* sp. nov. for strains D17^T (= KCTC 82958^T = JCM 34941^T) and D13 (= KCTC 92368), and *Deefgea tanakiae* sp. nov. for strain D25^T (= KCTC 82959^T = JCM 34942^T).

Keywords: *Deefgea*, *Deefgea piscis*, *Deefgea tanakiae*, Korean dark sleeper, *Odontobutis platycephala*, Kumgang fat minnow, *Rhynchocypris kumgangensis*, Korean oily bitterling, *Tanakia koreensis*

Introduction

Gut microbiota has an important role in host metabolism, immune system, digestion, and fitness (Yang *et al.*, 2018; Huan *et al.*, 2020; Zhou *et al.*, 2021). Although the gut microbial community of mammals is well known, that of wild fish remains largely unexplored (Kim *et al.*, 2021b). Hence, we investigated the gut microbiota of three Korean indigenous fish and isolated 67 bacterial strains belonging to six genera and 13 species. Among 67 strains, three putative novel strains were identified as two candidate novel species closely related to the genus *Deefgea* from the gut of the Korean dark sleeper (*Odontobutis platycephala*), Kumgang fat minnow (*Rhynchocypris kumgangensis*), and the Korean oily bitterling (*Tanakia koreensis*), respectively. The genus *Deefgea* was first identified as a member of the family *Chromobacteriaceae* belonging to the order *Neisseriales*, class *Betaproteobacteria*, and phylum *Pseudomonadota* by Stackebrandt *et al.* (2007). The genus currently consists of two validly published species: *D. rivuli* (Stackebrandt *et al.*, 2007) and *D. chitinilytica* (Chen *et al.*, 2010). These two species are characterized as being Gram-stain-negative, obligate aerobes or facultative aerobes, motile, and rod-shaped. Both species are positive for catalase and oxidase and contain Q-8 as the predominant ubiquinone. The genome sizes range from 3.4 to 3.7 Mb, and the DNA G + C contents range from 48.3% to 49.0%. *D. rivuli* WB 3.4-79^T and *D. chitinilytica* Nsw-4^T had been isolated from a hard-water sample of Westerhöfer Bach, Harz Mountains in Lower Saxony, Germany (Stackebrandt *et al.*, 2007), and from a water sample of Niao-Song Wetland Park, Taiwan (Chen *et al.*, 2010). Considering the overall isolation sources, the members of the genus *Deefgea* seem to be distributed in freshwater environments. Korean dark sleeper, Kumgang fat minnow, and the Korean oily bitterling are endemic freshwater species in the Korean peninsula. The Korean dark sleeper belonging to the order *Perciformes*, family *Odontobutidae*, has been known to inhabit most rivers in the Korean peninsula (Sohn *et al.*, 2018). Kumgang fat minnow and the Korean oily bitterling belong to the order *Cypriniformes*, family *Cyprinidae*, mainly inhabit the upper reaches of the Han River and distribute in the rivers flowing into the South Sea or the West Sea toward the south of Geumgang. (Lee *et al.*, 2008; Hwang *et al.*, 2013). In this study, we isolated three novel strains (D17^T, D13, and D25^T) during investigations of the gut mi-

[†]These authors contributed equally to this study.
*For correspondence. E-mail: baejw@khu.ac.kr; Tel.: +82-2-961-2312; Fax: +82-2-961-9155
[§]Supplemental material for this article may be found at https://doi.org/10.1007/s12275-022-2250-5.
Copyright ⓒ 2022, Author(s) under the exclusive license with the Microbiological Society of Korea

crobiota of the three fish using culture-dependent methods. We also reported the phylogenetic, genomic, physiological, morphological, and chemotaxonomic characteristics of these putative novel strains, suggesting that strains D17^T, D13, and D25^T represent two novel species of the genus *Deefgea*.

Materials and Methods

Bacterial isolation and deposition

Whole gut tissue and content samples of the Korean oily bitterling (*Tanakia koreensis*), Korean dark sleeper (*Odontobutis platycephala*), and Kumgang fat minnow (*Rhynchocypris kumgangensis*) were homogenized and then serially diluted to 10^{-1} to 10^{-4} with sterile phosphate-buffered saline (PBS). The diluted gut samples were individually spread on tryptic soy broth (TSB, Bacto) with 1.5% agar, marine broth (MB, Difco) with 1.5% agar, and Reasoner's 2A agar (R2A, Difco) and incubated at 30°C under aerobic conditions. Single colonies were collected during three subcultivations, and the obtained pure colonies were preserved at -80°C in glycerol stocks containing 40% (v/v) glycerol. The representative isolates were deposited at the Korean Collection for Type Cultures (KCTC) and the Japan Collection of Microorganisms (JCM). The accession numbers are KCTC 82958 and JCM 34941 for strain D17^T, KCTC 92368 for strain D13, and KCTC 82959 and JCM 34942 for strain D25^T.

Phylogenetic analyses based on 16S rRNA gene

To determine the taxonomic positions of strains D17^T, D13, and D25^T, phylogenetic analyses were performed based on the 16S rRNA gene sequences. We suspended a single colony of the three strains in the PCR PreMix (Bioneer) with bacteria-specific universal primers 27F and 1492R (Lane, 1991) and performed colony PCR using a C1000 Touch Thermal Cycler (Bio-Rad). The nearly full-length 16S rRNA gene sequences were assembled with 27F, 785F, 800R, and 1492R using the SeqMan Pro 5.0 software program (DNASTAR), and phylogenetically related species were selected using a bacterial identification service, which is available on the EzBioCloud server (Yoon *et al.*, 2017). Then, we aligned assembled sequences with the 16S rRNA gene sequences of closely related species using CLUSTAL W software (Thompson *et al.*, 1994). Phylogenetic trees were constructed based on the aligned sequences using neighbor-joining (NJ) (Saitou and Nei, 1987), maximum-likelihood (ML) (Felsenstein, 1981), and maximum-parsimony (MP) algorithms (Kluge and Farris, 1969), available in MEGA (version 7.0.26) software with 1,000 bootstrap replicates. *Moraxella lacunata* NBRC 102154^T was used as an outgroup.

Genome sequencing and analysis

To obtain the whole-genome sequences of strains D17^T, D13, and D25^T, we extracted the genomic DNA using the Qiagen MagAttract HMW DNA Kit. To purify extracted genomic DNA, we used a chloroform wash protocol of PacBio Guidelines. Then, a 20-kb library was prepared using the PacBio DNA Template Prep Kit 1.0, SMRT Cell 8Pac V3, and DNA Polymerase Binding Kit P6. The RS HGAP Assembly v3.0 software was used for *de novo* assembly (Chin *et al.*, 2013). To further validate the taxonomic positions of the three novel strains in the genus *Deefgea*, we constructed an up-to-date bacterial core gene (UBCG) tree (Na *et al.*, 2018) using the FastTree program (Price *et al.*, 2009). In order to elucidate the genomic relatedness, we calculated the digital DNA-DNA hybridization (dDDH) and the orthologous average nucleotide identity (OrthoANI) values using the Genome-to-Genome Distance Calculator (GGDC) (version 3.0) (http://ggdc.dsmz.de/) (Meier-Kolthoff *et al.*, 2013) and OAT software (Lee *et al.*, 2016), respectively. In addition, we also calculated the average amino acid identity (AAI) values based on MMseqs2 (AAIm) and produced an unweighted pair group method with arithmetic mean (UPGMA) dendrogram using the EzAAI tool (Kim *et al.*, 2021a). Using the Rapid Annotation using Subsystem Technology (RAST) server (https://rast.nmpdr.org/) (Aziz *et al.*, 2008) and IMG-Expert Review (IMG-ER) platform (https://img.jgi.doe.gov/) (Chen *et al.*, 2019), we annotated the genomes of strains D17^T, D13, D25^T, and closely related species. Using the TrueBac ID service (https://www.truebacid.com/) (Ha *et al.*, 2019), we identified genome-encoded antimicrobial resistance (AMR) genes and virulence factor (VF) genes. Carbohydrate-active enzyme (CAZyme) analysis was performed through a meta-server for automated carbohydrate-active enzyme annotation (dbCAN) (http://bcb.unl.edu/dbCAN2/index.php) (Zhang *et al.*, 2018) with HMMER, DIAMOND, and Hotpep tools. To identify orthologous protein sequence groups, we performed a pan-genome analysis using the OrthoMCL software (version 2.0) (Fischer *et al.*, 2011) available on the KBase server (https://www.kbase.us/) (Arkin *et al.*, 2018).

Comparative analyses

We obtained each type strain of *D. rivuli* WB 3.4-79^T and *D. chitinilytica* Nsw-4^T from the German Collection of Microorganisms (Deutsche Sammlung von Mikroorganismen und Zellkulturen GmbH, DSMZ) and then compared the phenotypic characteristics of those type strains with strains D17^T, D13, and D25^T. To perform comparative genome analyses, we obtained publicly available genomic data of *D. rivuli* WB 3.4-79^T and *D. chitinilytica* Nsw-4^T from the National Center for Biotechnology Information (NCBI) database. Pairwise comparisons of OrthoANI, dDDH, and AAIm values were also performed.

Growth conditions and morphological analyses

To identify the optimal growth conditions for the strains D17^T, D13, and D25^T, we cultured the strains under various temperatures (4, 10, 15, 20, 25, 30, 37, 45, 55, and 65°C), various pH (4.0, 5.0, 6.0, 7.0, 8.0, 9.0, 10.0, and 11.0) buffered by 10 mM 2-(*N*-morpholino)-ethanesulfonic acid (MES, for pH 4.0–6.0), 10 mM *N*-tris(hydroxymethyl)-methyl-3-aminopropanesulfonic acid (TAPS, for pH 7.0–9.0), or 10 mM Na_2HPO_4 (for pH 10.0–11.0), and various NaCl concentrations (0, 0.5, 1.0, 1.5, 2.0, 3.0, 4.0, 5.0, 6.0, 7.0, 8.0, 10, and 12% w/v NaCl) in TSB. After incubation for 1, 2, and 7 days under the above conditions, the optimal growth conditions were identified by measuring the turbidity of the media at 600 nm (OD_{600}) using a Synergy Mx spectrophotometer (Bio-

Tek). Through this analysis, we identified optimal growth conditions of the three strains and incubated the strains for 2 days under the optimal growth conditions for following analyses. To determine the oxygen dependence, we incubated the three strains on TSB with 1.5% agar (TSA) for 7 days in a Bactron II-2 anaerobic chamber (Sheldon Manufacturing) filled with N_2 (90%), CO_2 (5%), and H_2 (5%). Additionally, Gram-staining was performed using a Gram-stain kit (bioMérieux), and cells were observed under a light microscope (Eclipse 50i; Nikon). Cell morphologies were observed using an energy-filtering transmission electron microscope (LIBRA 120; Zeiss). The motility of cells was tested using semi-solid TSB containing 0.4% agar (Lee *et al.*, 2020).

Biochemical characterization

To determine the biochemical characteristics, including enzymatic activity, assimilation reaction, and utilization of carbon sources, we used API ZYM, API 20E, API 20NE, and API 50CH test strips (bioMérieux), and GEN III MicroPlate (Biolog). Catalase activity was assessed by observation of bubbles in the presence of 3% (v/v) hydrogen peroxide solution (Lee *et al.*, 2019). Oxidase activity was assessed by observation of indophenol blue after adding 1% (w/v) tetramethyl *p*-phenylenediamine solution (bioMérieux).

Chemotaxonomic characteristics

The cellular fatty acids of strains D17^T, D13, D25^T, and the closely related reference strains were extracted following the protocol of the Sherlock Microbial Identification System (MIDI) operating manual (version 4.5). The extracted fatty acids were separated and analyzed by gas chromatography (6890 GC system; Agilent Technologies) with the Microbial Identification software package (Sherlock version 6.3) based on the TSBA6 library (Sasser, 1990). Freeze-dried cell harvests were used to extract the bacterial quinones and polar lipids. Isoprenoid quinones were extracted following a previously published method performed in the dark (Collins and Jones, 1981) and analyzed using a reverse-phase HPLC instrument (Younglin) (Hiraishi *et al.*, 1996). The polar lipids of strains D17^T, D13, and D25^T were extracted according to the protocols previously described (Minnikin *et al.*, 1984). The extracted polar lipids were analyzed through two-dimensional

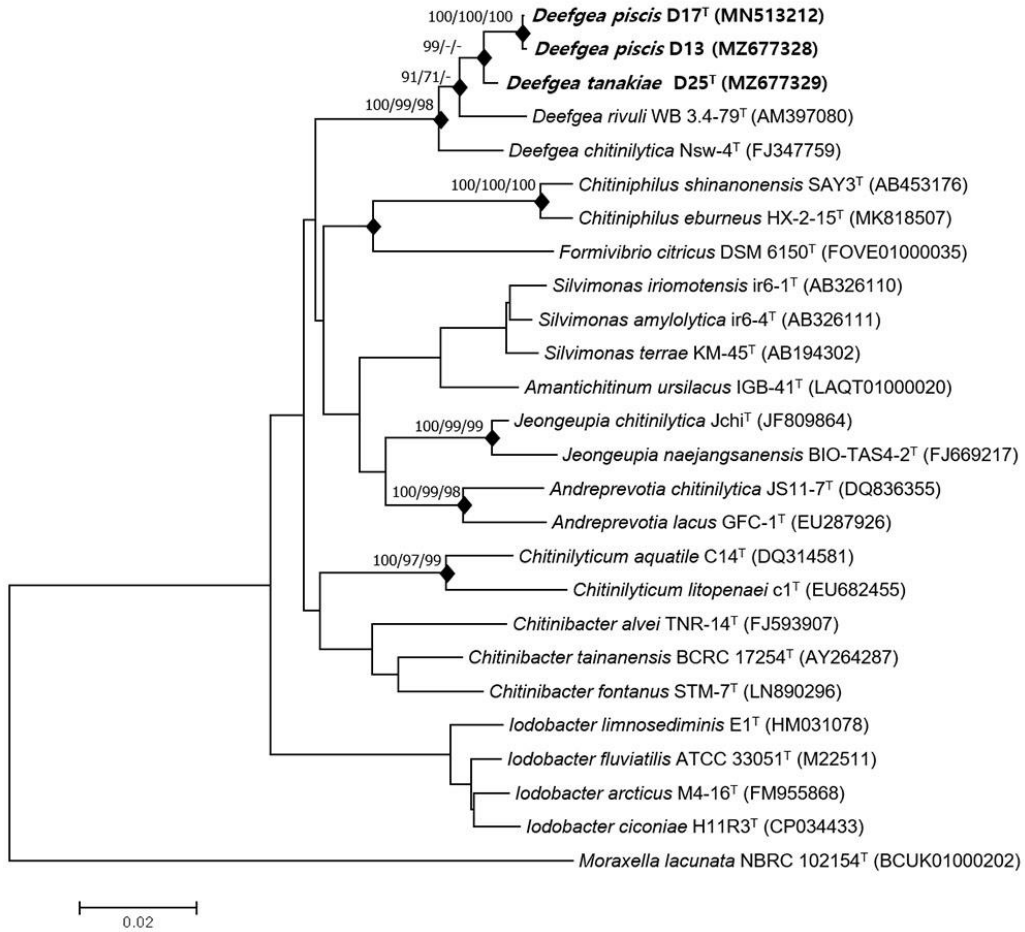

Fig. 1. The 16S rRNA gene-based NJ phylogenetic consensus tree of *Deefgea piscis* D17^T, *D. piscis* D13, *D. tanakiae* D25^T, and the closely related species affiliated to the order *Neisseriales*. *Moraxella lacunata* NBRC 102154^T was used as an outgroup. Filled diamonds indicate that overlapping nodes were also generated with ML and MP algorithms. The bootstrap value (NJ/ML/MP) algorithms based on 1,000 replications are presented at the nodes. Only bootstrap values > 70% are marked on the corresponding nodes. Bar, 0.02 substitutions per nucleotide position.

Table 1. The genomic features of *Deefgea piscis* D17^T, *D. piscis* D13, *D. tanakiae* D25^T, and the closely related species
Strains: 1, *D. piscis* D17^T; 2, *D. piscis* D13; 3, *D. tanakiae* D25^T; 4, *D. rivuli* WB 3.4-79^T; 5, *D. chitinilytica* Nsw-4^T.

Feature	1	2	3	4	5
NCBI accession number	GCA_013284055.1	GCA_01966578.1	GCA_019665765.1	GCA_000620145.1	GCA_016881405.1
Numbers of contig	3	1	1	29	24
Genome size (bp)	3,428,786	3,575,158	3,557,673	3,711,979	3,402,224
G + C content (%)	48.2	48.1	48.1	49.0	48.3
Numbers of total genes	3,265	3,458	3,420	3,468	3,220
Numbers of rRNA genes (5S/16S/23S)	24 (8/8/8)	21 (7/7/7)	21 (7/7/7)	14 (7/3/4)	2 (0/1/1)
Numbers of tRNA genes	81	78	80	58	64

thin-layer chromatography (TLC) using silica gel 60 F_{254} plates (Merck). The extracted polar lipids were spotted on the edge of TLC plates and subsequently separated by two types of solvent. We used a mixture of chloroform:methanol:distilled water (DW) (65:25:4, v/v/v) and a mixture of chloroform: acetic acid:methanol:DW (80:15:12:4, v/v/v/v) for the first and second dimensions of separation, respectively. Three types of spray reagent were used to detect polar lipid spots on TLC plates: 10% ethanolic phosphomolybdic acid (Merck) for total lipid, molybdenum blue spray reagent (Sigma-Aldrich) for phospholipid (PL), and ninhydrin (Merck) reagent for aminolipid (AL) detection. To further clarify PL spots, one-dimensional TLC was performed with a chloroform:acetic acid: methanol:DW (50:6:6:1, v/v/v/v) mixture. The standard solutions of phosphatidylethanolamine (PE), phosphatidylglycerol (PG), phosphatidylcholine (PC), phosphatidylinositol (PI), phosphatidylserine (PS), and diphosphatidylglycerol (DPG) were used to define each PL spot on the TLC plates.

Accession numbers

The DDBJ/ENA/GenBank accession numbers for the 16S rRNA gene sequences of strains D17^T, D13, and D25^T are MN513212, MZ677328, and MZ677329, respectively. The DDBJ/ENA/GenBank accession numbers for the whole-genome sequences of strains D17^T, D13, and D25^T are GCA_013284055.1, GCA_019665785.1, and GCA_019665765.1, respectively.

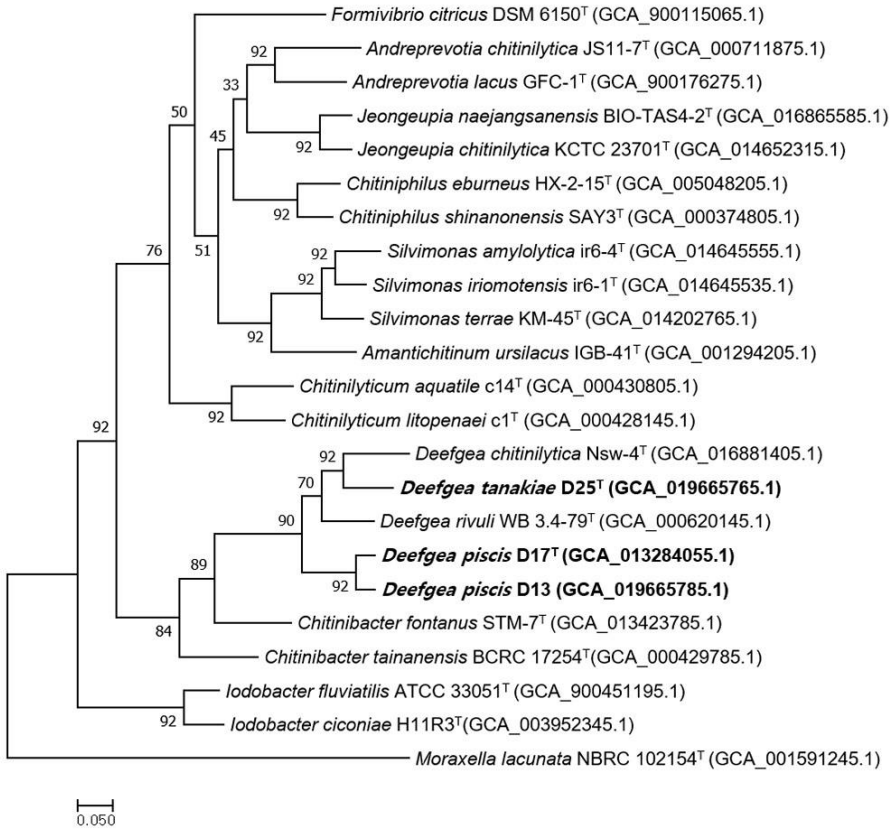

Fig. 2. The UBCG tree of *Deefgea piscis* D17^T, *D. piscis* D13, *D. tanakiae* D25^T, and the closely related species. *Moraxella lacunata* NBRC 102154^T was used as an outgroup. The numbers on nodes are gene support index (GSI) values indicating the number of single-gene trees supporting the branch. Bar, 0.05 substitutions per nucleotide position.

Results

Phylogenetic and genomic analyses

Based on comparisons of nearly full-length 16S rRNA gene sequences, the strains D17^T, D13, and D25^T were identified as members of the genus *Deefgea*, family *Chromobacteriaceae*, order *Neisseriales*, class *Betaproteobacteria*, and phylum *Pseudomonadota*. Strains D17^T and D13 were most closely related to *D. rivuli* WB 3.4-79^T (98.0% and 97.9%, respectively) and subsequently closely related to *D. chitinilytica* Nsw-4^T (96.8% and 96.7%, respectively), while strain D25^T was most closely related to *D. chitinilytica* Nsw-4^T (98.2%) and subsequently closely related to *D. rivuli* WB 3.4-79^T (98.0%). Strain D17^T and D13 showed 99.9% of 16S rRNA gene sequence similarity. In a phylogenetic tree based on 16S rRNA gene sequences, the three novel strains formed a monophyletic clade with *D. rivuli* WB 3.4-79^T and *D. chitinilytica* Nsw-4^T (Fig. 1).

Whole-genome sequences of strains D17^T, D13, and D25^T contained 3,428,786 bp with a 48.2% DNA G+C content, 3,575,158 bp with a 48.1% DNA G + C content, and 3,557,673 bp with a 48.1% DNA G + C content, respectively (Table 1). Strains D17^T, D13, and D25^T harbored a total of 3,265, 3,458, and 3,420 genes, respectively. Strains D17^T, D13, and D25^T had 24 rRNA genes and 81 tRNA genes, 21 rRNA genes and 78 tRNA genes, and 21 rRNA genes and 80 tRNA genes, respectively. Again, in the UBCG tree based on genome sequences, the strains D17^T, D13, and D25^T formed a monophyletic clade with *D. rivuli* WB 3.4-79^T and *D. chitinilytica* Nsw-4^T (Fig. 2). To determine the genome sequence similarities, we calculated OrthoANI, dDDH, and AAIm values (see Supplementary data Table S1). A dendrogram based on the AAIm matrix is presented in Supplementary data Fig. S1. The genomes of *D. rivuli* WB 3.4-79^T and *D. chitinilytica* Nsw-4^T showed the highest similarities to that of strain D25^T: 80.1% OrthoANI, 23.3% dDDH, and 85.9% AAIm values, and 82.4% OrthoANI, 25.1% dDDH, and 89.5% AAIm values, respectively, while these genomes showed lower similarities to that of strain D17^T: 77.8% OrthoANI, 21.9% dDDH, and 81.6% AAIm values, and 76.6% OrthoANI, 21.4% dDDH, and 80.8% AAIm values, respectively. These values were much lower than the species demarcation thresholds (95–96% for ANI, 70% for dDDH, and 95% for AAI values) (Luo *et al.*, 2014; Chun *et al.*, 2018). Thus, these novel strains had a distinct identity from the reference strains proposed in the present study. Strain D17^T and D13 showed the highest similarities in complete genome sequences (91.8% of OrthoANI, 45.1% of dDDH, and 95.9% AAIm values). Considering the 16S rRNA gene and complete genome sequences similarities, D17^T and D13 were assigned as the same species.

Using the RAST server, we annotated the genome sequences of strain D17^T, strain D13, strain D25^T, *D. rivuli* WB 3.4-79^T, and *D. chitinilytica* Nsw-4^T. Then, annotated genes were clustered into several subsystems. The major subsystems associated with all the compared strains were 'cofactors, vitamins, prosthetic groups, pigments', 'protein metabolism', 'amino acids and derivatives', and 'carbohydrates' (Supplementary data Table S2). By referring to the Clusters of Orthologous Groups (COGs) database, a total of 2,590, 2,689, and 2,692 protein-coding genes of strains D17^T, D13, and D25^T were assigned to COG functional categories, respectively (Supplementary data Fig. S2 and Table S3). Strains D17^T, D13, and D25^T had a high proportion of COGs with genes related to 'amino acid transport and metabolism (code E)', 'carbohydrate transport and metabolism (G)', 'cell motility (N)', 'cell wall/membrane/envelope biogenesis (M)', 'coenzyme transport and metabolism (H)', 'energy production and conversion (C)', 'inorganic ion transport and metabolism (P)', 'posttranslational modification, protein turnover, chaperones (O)', 'replication, recombination and repair (L)', 'signal transduction mechanisms (T)', 'transcription (K)', and 'translation, and ribosomal structure and biogenesis (J)'. These distribution patterns were also observed in two reference species. Compared with the other strains, strain D17^T had the highest proportion of COGs related to 'cell wall/membrane/envelope biogenesis (M)' and the lowest proportion of COGs related to 'secondary metabolites biosynthesis, transport, and catabolism (Q)', while strain D13 had the highest proportion of COGs related to 'mobilome: prophages, transposons (X)' and the lowest proportion of COGs related to 'inorganic ion transport and metabolism (P)'. We performed pan-genome analysis to arrange proteins into orthologous protein clusters by categorizing the protein-coding genes as core, singleton, and accessory genes (Supplementary data Fig. S3 and Table S4). All the described strains shared 2,200 homologous gene clusters. Strain D17^T harbored 2,217 (72.3%) core genes and 202 (6.6%) singleton genes, while strain D13 harbored 2,241 (69.1%) core genes and 328 (10.1%) singleton genes. Strain D25^T harbored 2,241 (69.9%) core genes and 290 (9.1%) singleton genes. Additionally, we compared their AMR and VF genes. The *bla*$_{OXA}$ (antibiotic resistance ontology, ARO ID: ARO3000075) gene family was found in all the compared strains, while the *ampC* (ARO ID: ARO3000076) gene family was only found in strain D17^T (Supplementary data Table S5). Strains D17^T, D13, and D25^T contained 31, 26, and 36 VF-like genes, respectively (Supplementary data Table S6). All the compared strains commonly contained 12 VF-like genes, including those encoding Hsp60, 60K heat shock protein HtpB (virulence factors database, VFDB ID: VFG001855), twitching ATPase TapT (VFDB ID: VFG038463), type IV pilus twitching motility protein PilT (VFDB ID: VFG042870), ATP-dependent Clp protease proteolytic subunit ClpP (VFDB ID: VFG000077), twitching motility protein PilT (VFDB ID: VFG000232), twitching motility protein PilT (VFDB ID: VFG001223), isocitrate lyase Icl (isocitrase) (isocitratase) ICL (VFDB ID: VFG001381), acyl carrier protein AcpXL (VFDB ID: VFG011430), *Coxiella* Dot/Icm type IVB secretion system translocated effector CBU_1566 (VFDB ID: VFG039536), phosphoglucomutase PGM (VFDB ID: VFG002220), general secretion pathway protein E XcpR (VFDB ID: VFG000182), and twitching motility protein PilT2 (VFDB ID: VFG006199). Three VF-like genes, namely those encoding the chemotaxis regulatory protein CheY (VFDB ID: VFG043206), flagellar motor protein MotA (VFDB ID: VFG043213), and twitching motility protein PilU (VFDB ID: VFG001224), were also dominantly found in the compared strains. Specifically, two VF-like genes, namely those encoding the 2-dehydro-3-deoxyphosphooctonate aldolase KdsA (VFDB ID: VFG013465) and outer membrane protein A OmpA (VFDB ID: VFG001443), were present only in strain D17^T. Based on the genome sequences of strains D17^T, D13, and D25^T, 85, 93, and

100 proteins were annotated as CAZymes, respectively, by at least three tools provided at the dbCAN meta-server (Supplementary data Table S7). Of the six functional family domains in strains D17^T, D13, and D25^T, the most abundant families were glycosyltransferases (38, 39, and 39 domains, respectively), followed by glycoside hydrolases (28, 30, and 35 domains, respectively), carbohydrate-binding modules (15, 18, and 20 domains, respectively), carbohydrate esterases (one, two, and five domains, respectively), auxiliary activity (one, two, and one domain, respectively), and polysaccharide lyases (two, two, and zero domains, respectively).

Physiological, morphological, and biochemical features

Strain D17^T grew on TSA at the range of 10–30°C, at pH 7.0–9.0, and in the presence of 0–2.0% (w/v) NaCl. The optimal growth of strain D17^T was observed on TSA at 20–25°C and pH 8.0 and in the presence of 0.5–1.0% (w/v) NaCl. Strain D13 grew on TSA at the range of 10–25°C and pH 6.0–9.0 and in the presence of 0–2.0% (w/v) NaCl. The optimal growth of strain D13 was observed on TSA at 25°C and pH 9.0 and in the presence of 0.5% (w/v) NaCl. Strain D25^T grew on TSA at the range of 10–25°C, at pH 7.0–9.0, and in the presence of 0–1.5% (w/v) NaCl. The optimal growth of strain D25^T was observed on TSA at 25°C and pH 8.0 and in the presence of 0–0.5% (w/v) NaCl. Given that the strains D17^T, D13, and D25^T grew well on TSA, the following biochemical analyses of these strains and the reference strains were performed using cells cultivated on TSA under the same growth conditions; 25°C and pH 8.0 and in the presence of 0.5% (w/v) NaCl. Strains D17^T, D13, and D25^T were facultative anaerobes, Gram-stain-negative, and rod-shaped. Strains D17^T and D13 were non-motile and non-flagellated, while D25^T was motile and had a single polar flagellum (Supplementary data Fig. S4). The sizes of the cells are detailed in the description. Colonies of strains D17^T, D13, and D25^T were ivory-colored, circular, opaque, and smooth, with raised elevation

Table 2. Differential biochemical characteristics of *Deefgea piscis* D17^T, *D. piscis* D13, *D. tanakiae* D25^T, and the closely related species

All strains were positive for the following: utilization of glucuronamide as a sole carbon source (Biolog GEN III); chemical tolerance to rifamycin SV (Biolog GEN III); acid production from ribose, glucose, fructose, *N*-acetyl-glucosamine, esculin, and gluconate (API 50CHB); enzymatic activities of leucine arylamidase, naphthol-AS-BI-phosphohydrolase, and acid phospatase (API ZYM, API 20NE); assimilation of potassium gluconate (API 20NE); and oxidase and catalase. All strains were negative for the following: utilization of dextrin, D-galactose, D-trehalose, α-keto-butyric acid, D-melibiose, D-salicin, α-D-lactose, gentiobiose, *N*-acetyl-D-galactosamine, D-raffinose, D-cellobiose, γ-amino-butryic acid, stachyose, β-methyl-D-glucoside, glycerol, acetoacetic acid, D-fucose, L-fucose, L-rhamnose, L-arginine, D-turanose, D-galacturonic acid, L-galactonic acid lactone, *N*-acetyl neuraminic acid, Tween 40, acetic acid, methyl pyruvate, and L-lactic acid as a sole carbon source (Biolog GEN III); chemical tolerance to troleandomycin, D-serine, and lithium chloride (Biolog GEN III); acid production from erythritol, D-xylose, L-xylose, adonitol, methyl-β-D-xylopyranoside, sorbose, dulcitol, inositol, mannitol, sorbitol, methyl-α-D-mannopyranoside, methyl-α-D-glucoside, amygdalin, arbutin, inulin, melezitose, starch, glycogen, xylitol, D-tagatose, D-arabitol, L-arabitol, and 2-keto-gluconate (API 50CHB); enzymatic activities of α-chymotrpsin, α-galactosidase, β-galactosidase, β-glucosidase, β-glucuronidase, and arginine dihydrolase (API ZYM, 20NE); and assimilation of maltose and arabinose (API 20NE).

Strains: 1, *D. piscis* D17^T; 2, *D. piscis* D13; 3, *D. tanakiae* D25^T; 4, *D. rivuli* WB 3.4-79^T; 5, *D. chitinilytica* Nsw-4^T. Data for growth conditions of *D. rivuli* WB 3.4-79^T and *D. chitinilytica* Nsw-4^T are from Stackebrandt *et al.* (2007) and Chen *et al.* (2010), respectively. +, Positive; w, weakly positive; –, negative.

Characteristic	1	2	3	4	5
Growth conditions:					
Temperature range (°C)	10–30	10–25	10–25	4–32	15–37
NaCl range (%, w/v)	0–2	0–2	0–1.5	0–1	0–2
pH range (pH)	7–9	6–9	7–9	5.8–8.5	6–8
Utilization as a sole carbon source (Biolog GEN III):					
D-Maltose	–	–	–	w	+
N-Acetyl-β-D-mannosamine	+	–	–	–	–
Sucrose, pectin	–	–	–	+	–
D-Glucose-6-PO4, D-fructose-6-PO4	+	w	w	w	w
D-Glucuronic acid	–	–	–	–	w
Chemical tolerance (Biolog GEN III):					
Potassium tellurite, minocycline, sodium butyrate	+	w	w	–	w
1% Sodium lactate	–	–	–	–	w
Fusidic acid	+	–	–	–	–
Aztreonam	+	+	w	+	w
Niaproof 4	+	w	–	–	+
Lincomycin	+	w	+	+	+
Sodium bromate	+	w	w	–	w
Vancomycin	+	w	+	+	+
Tetrazolium violet	–	w	–	+	w
Acid production from (API 50CHB):					
Mannose	+	+	+	–	+
D-Lyxose	–	–	w	–	–
5-Keto-gluconate	–	w	w	w	w
Enzymatic activities of (API ZYM, 20NE):					
Esterase lipase (C8)	w	–	–	–	w
Esterase (C4)	w	w	w	–	+

and an undulate margin on TSA. The differential biochemical features of all the compared strains are presented in Table 2, and the phenotypic features of strains D17^T, D13, and D25^T are presented in the description.

Chemotaxonomic characterization

The major fatty acids (> 20%) of strains D17^T, D13, and D25^T were $C_{16:0}$ and summed feature 3 ($C_{16:1}$ *ω7c* and/or $C_{16:1}$ *ω6c*). The detailed fatty acid profiles of the strains are presented in Table 3. The polar lipids of strain D17^T were composed of one PE, one PG, one DPG, one aminophospholipid (APL), two unidentified ALs, one unidentified PL, and one unidentified lipid. The polar lipids of strain D13 contained one PE, one PG, one DPG, two unidentified APLs, one unidentified AL, three unidentified PLs, and two unidentified lipids. The polar lipids of strain D25^T contained one PE, one PG, one DPG, two unidentified APLs, three unidentified PLs, and two unidentified lipids but did not contain AL. Strains D17^T, D13, and D25^T contained PE and PG as major polar lipids, as observed in other *Deefgea* species (Supplementary data Fig. S5). Strains D17^T, D13, and D25^T contained ubiquinone Q-8 as a predominant respiratory quinone, as observed in other *Deefgea* species (Supplementary data Fig. S6).

Taken together, strains D17^T, D13, and D25^T were Gram-stain-negative, rod-shaped, facultative anaerobes and contained $C_{16:0}$ and $C_{16:1}$ *ω7c* as major fatty acids, ubiquinone Q-8 as a predominant respiratory quinone, and PE and PG as major polar lipids, as observed in other *Deefgea* species. However, these strains showed distinct differences in phenotypic and genomic features compared to *D. rivuli* WB 3.4-79^T and *D. chitinilytica* Nsw-4^T. Furthermore, D17^T and D13 were non-motile and non-flagellated, while D25^T was motile and had one flagellum, as observed in other *Deefgea* species. Therefore, the overall phylogenetic, genomic, chemotaxonomic, physiological, biochemical, and phenotypic findings suggest that strains D17^T, D13, and D25^T represent two novel species within the genus *Deefgea*. We propose the name *D. piscis* sp. nov. for strains D17^T and D13, and *D. tanakiae* sp. nov. for strain D25^T.

Table 3. Fatty acid compositions (%) of *Deefgea piscis* D17^T, *D. piscis* D13, *D. tanakiae* D25^T, and the type strains of the reference species in the genus *Deefgea*

Strains: 1, *D. piscis* D17^T; 2, *D. piscis* D13; 3, *D. tanakiae* D25^T; 4, *D. rivuli* WB 3.4-79^T; 5, *D. chitinilytica* Nsw-4^T. All data were obtained in this current study. Symbol: TR, trace (< 1%); –, not detected.

Fatty acid (%)	1	2	3	4	5
Saturated straight-chain					
$C_{12:0}$	5.47	5.36	5.05	2.90	2.72
$C_{14:0}$	1.67	2.07	1.45	2.36	3.03
$C_{16:0}$	32.21	39.68	25.70	27.10	21.96
$C_{18:0}$	TR	TR	1.91	TR	TR
Saturated branched-chain					
$C_{12:0}$ 3OH	3.47	3.15	3.18	2.69	2.20
$C_{16:0}$ 3OH	TR	1.06	1.23	TR	TR
Unsaturated straight-chain					
$C_{15:1}$ *ω6c*	–	TR	2.05	TR	TR
Summed features					
3	45.90	43.80	51.47	56.02	54.78
8	6.75	1.57	3.70	4.64	10.11

* Summed features were used when two or three fatty acids could not be separated by the Microbial Identification System. Summed feature 3 was comprised of $C_{16:1}$ *ω7c* and/or $C_{16:1}$ *ω6c*. Summed feature 8 was comprised of $C_{18:1}$ *ω7c* and/or $C_{18:1}$ *ω6c*.

Description of *Deefgea piscis* sp. nov.

Deefgea piscis (pis'cis. L. gen. n. *piscis*, of a fish, from which the strain was first isolated).

Cells are Gram-stain-negative, facultative anaerobe, non-motile, non-flagellated, and rod-shaped (1.0–2.0 μm × 2.5–5.1 μm). Colonies are ivory-colored, circular form, opaque, smooth texture, and raised elevation with an undulate margin on TSA after 48 h. Cells grow at 10–30°C and pH 7.0–9.0 and in the presence of 0–2.0% (w/v) NaCl. Optimal growth occurs at 20–25°C and pH 8.0 and in the presence of 0.5–1.0% (w/v) NaCl. Cells are positive for oxidase and catalase and utilize glucuronamide, *N*-acetyl-*β*-D-mannosamine, D-glucose-6-PO_4, and D-*α*-6-PO_4 as a sole carbon source (Biolog GEN III). Cells are tolerant to potassium tellurite, minocycline, rifamycin SV, fusidic acid, aztreonam, sodium butyrate, Niaproof 4, lincomycin, sodium bromate, and vancomycin (Biolog GEN III), and are positive for nitrate reduction and glucose fermentation, and enzyme activities of leucine arylamidase, esterase lipase (C8), naphthol-AS-BI-phosphohydrolase, esterase (C4), and acid phosphatase (API ZYM, 20NE). Cells can assimilate potassium gluconate (API 20NE). Cells can produce acid from mannose, ribose, glucose, fructose, *N*-acetyl-glucosamine, esculin, and gluconate (API 50CHB). Cells are unable to utilize dextrin, D-galactose, D-trehalose, D-maltose, *α*-keto-butyric acid, D-melibiose, D-salicin, sucrose, *α*-D-lactose, gentiobiose, *N*-acetyl-D-galactosamine, D-raffinose, D-cellobiose, pectin, *γ*-aminobutyric acid, stachyose, *β*-methyl-D-glucoside, glycerol, acetoacetic acid, D-fucose, L-fucose, L-rhamnose, L-arginine, D-turanose, D-galacturonic acid, L-galactonic acid lactone, *N*-acetyl neuraminic acid, Tween 40, acetic acid, D-glucuronic acid, methyl pyruvate, and L-lactic acid as a sole carbon source (Biolog GEN III). Cells are not tolerant to 1% sodium lactate, troleandomycin, D-serine, lithium chloride, and tetrazolium violet (Biolog GEN III). Cells are negative for enzyme activities of *α*-chymotrypsin, *α*-galactosidase, *β*-galactosidase, *β*-glucosidase, *β*-glucuronidase, and arginine dihydrolase (API ZYM, 20NE), and indole production (API 20NE). Cells do not assimilate maltose and arabinose (API 20NE). Cells do not produce acid from 5-keto-gluconate, erythritol, D-xylose, L-xylose, adonitol, methyl-*β*-D-xylopyranoside, sorbose, dulcitol, inositol, mannitol, sorbitol, methyl-*α*-D-mannopyranoside, methyl-*α*-D-glucoside, amygdalin, arbutin, inulin, melezitose, starch, glycogen, xylitol, D-lyxose, D-tagatose, D-arabitol, L-arabitol, and 2-keto-gluconate (API 50CHB). The major fatty acids are $C_{16:0}$ and summed feature 3 ($C_{16:1}$ *ω7c* and/or $C_{16:1}$ *ω6c*), while ubiquinone Q-8 is a predominant respiratory quinone. Strain D17^T contains one PE, one PG, one DPG, one APL, two unidentified ALs, one unidentified PL, and one unidentified lipid. The genomic DNA G + C content is 48.2%.

Type strain D17^T (= KCTC 82958^T = JCM 34941^T) was isolated from the gut of the Korean dark sleeper *Odontobutis platycephala*. The DDBJ/ENA/GenBank accession numbers for the 16S rRNA gene sequence and genome sequences of strain D17^T are MN513212 and GCA_013284055.1, respectively.

Description of *Deefgea tanakiae* sp. nov.

Deefgea tanakiae (ta.na'ki.ae. N.L. gen. n. *tanakiae*, of *Tanakia*, from which the strain was first isolated).

Cells are Gram-stain-negative, facultative anaerobe, motile, one-flagellated, and rod-shaped (1.0–1.1 μm × 2.5–3.0 μm). Colonies are ivory-colored, circular form, opaque, smooth texture, and raised elevation with an undulate margin on TSA after 48 h. Cells grow at 10–25°C and pH 7.0–9.0 and in the presence of 0–2.0% (w/v) NaCl. Optimal growth occurs at 25°C and pH 8.0 and in the presence of 0–0.5% (w/v) NaCl. Cells are positive for oxidase and catalase and utilize glucuronamide, D-glucose-6-PO_4, and D-α-6-PO_4 as a sole carbon source (Biolog GEN III). Cells are tolerant to potassium tellurite, minocycline, rifamycin SV, aztreonam, sodium butyrate, lincomycin, sodium bromate, and vancomycin (Biolog GEN III), and are positive for nitrate reduction and glucose fermentation, and enzymatic activities of leucine arylamidase, naphthol-AS-BI-phosphohydrolase, esterase (C4), and acid phosphatase (API ZYM, 20NE). Cells can assimilate potassium gluconate (API 20NE). Cells can produce acid from mannose, ribose, glucose, fructose, *N*-acetyl-glucosamine, esculin, D-lyxose, gluconate, and 5-keto-gluconate (API 50CHB). Cells are unable to utilize dextrin, D-galactose, D-trehalose, D-maltose, *N*-acetyl-β-D-mannosamine, α-keto-butyric acid, D-melibiose, D-salicin, sucrose, α-D-lactose, gentiobiose, *N*-acetyl-D-galactosamine, D-raffinose, D-cellobiose, pectin, γ-amino-butyric acid, stachyose, β-methyl-D-glucoside, glycerol, acetoacetic acid, D-fucose, L-fucose, L-rhamnose, L-arginine, D-turanose, D-galacturonic acid, L-galactonic acid lactone, *N*-acetyl neuraminic acid, Tween 40, acetic acid, D-glucuronic acid, methyl pyruvate, and L-lactic acid as a sole carbon source (Biolog GEN III). Cells are not tolerant to 1 % sodium lactate, troleandomycin, D-serine, fusidic acid, Niaproof 4, lithium chloride, and tetrazolium violet (Biolog GEN III). Cells are negative for enzyme activities of α-chymotrypsin, α-galactosidase, β-galactosidase, β-glucosidase, β-glucuronidase, esterase lipase (C8), and arginine dihydrolase (API ZYM, 20NE), and indole production (API 20NE). Cells do not assimilate maltose and arabinose (API 20NE). Cells do not produce acid from erythritol, D-xylose, L-xylose, adonitol, methyl-β-D-xylopyranoside, sorbose, dulcitol, inositol, mannitol, sorbitol, methyl-α-D-mannopyranoside, methyl-α-D-glucoside, amygdalin, arbutin, inulin, melezitose, starch, glycogen, xylitol, D-tagatose, D-arabitol, L-arabitol, and 2-keto-gluconate (API 50CHB). The major fatty acids are $C_{16:0}$ and summed feature 3 ($C_{16:1}$ $\omega7c$ and/or $C_{16:1}$ $\omega6c$), while ubiquinone Q-8 is a predominant respiratory quinone. Strain D25^T contains one PE, one PG, one DPG, two unidentified APLs, three unidentified PLs, and two unidentified lipids. The genomic DNA G + C content is 48.1%.

Type strain D25^T (= KCTC 82959^T = JCM 34942^T) was isolated from the gut of the Korean oily bitterling *Tanakia koreensis*. The DDBJ/ENA/GenBank accession numbers for the 16S rRNA gene sequence and genome sequences of strain D25^T are MZ677329 and GCA_019665765.1, respectively.

Acknowledgements

We are grateful for the checking the species epithet by Dr. Aharon Oren (The Hebrew University of Jerusalem, Israel). This work was supported by grants from the Mid-Career Researcher Program (NRF-2020R1A2C3012797) through the National Research Foundation of Korea (NRF) and the National Institute of Biological Resources (NIBR201902111) funded by the Ministry of Environment of Korea (MOE).

Conflict of Interest

The authors declare that there are no conflicts of interest.

Ethical Statement

All sampling conducted in this study was approved by the Institutional Animal Care and Use Committee of Kyung Hee University (Permit number: KHUASP(SE)-18-048) and complied with the guidelines of the Committee.

References

Arkin, A.P., Cottingham, R.W., Henry, C.S., Harris, N.L., Stevens, R.L., Maslov, S., Dehal, P., Ware, D., Perez, F., Canon, S., *et al.* 2018. KBase: the United States department of energy systems biology knowledgebase. *Nat. Biotechnol.* **36**, 566–569.

Aziz, R.K., Bartels, D., Best, A.A., DeJongh, M., Disz, T., Edwards, R.A., Formsma, K., Gerdes, S., Glass, E.M., Kubal, M., *et al.* 2008. The RAST Server: rapid annotations using subsystems technology. *BMC Genomics* **9**, 75.

Chen, I.M.A., Chu, K., Palaniappan, K., Pillay, M., Ratner, A., Huang, J., Huntemann, M., Varghese, N., White, J.R., Seshadri, R., *et al.* 2019. IMG/M v. 5.0: an integrated data management and comparative analysis system for microbial genomes and microbiomes. *Nucleic Acids Res.* **47**, D666–D677.

Chen, W.M., Chung, Y.N., Chiu, T.F., Cheng, C.Y., Arun, A.B., and Sheu, S.Y. 2010. *Deefgea chitinilytica* sp. nov., isolated from a wetland. *Int. J. Syst. Evol. Microbiol.* **60**, 1450–1453.

Chin, C.S., Alexander, D.H., Marks, P., Klammer, A.A., Drake, J., Heiner, C., Clum, A., Copeland, A., Huddleston, J., Eichler, E.E., *et al.* 2013. Nonhybrid, finished microbial genome assemblies from long-read SMRT sequencing data. *Nat. Methods* **10**, 563–569.

Chun, J., Oren, A., Ventosa, A., Christensen, H., Arahal, D.R., da Costa, M.S., Rooney, A.P., Yi, H., Xu, X.W., De Meyer, S., *et al.* 2018. Proposed minimal standards for the use of genome data for the taxonomy of prokaryotes. *Int. J. Syst. Evol. Microbiol.* **68**, 461–466.

Collins, M.D. and Jones, D. 1981. Distribution of isoprenoid quinone structural types in bacteria and their taxonomic implication. *Microbiol. Rev.* **45**, 316–354.

Felsenstein, J. 1981. Evolutionary trees from DNA sequences: a maximum likelihood approach. *J. Mol. Evol.* **17**, 368–376.

Fischer, S., Brunk, B.P., Chen, F., Gao, X., Harb, O.S., Iodice, J.B., Shanmugam, D., Roos, D.S., and Stoeckert, C.J.Jr. 2011. Using OrthoMCL to assign proteins to OrthoMCL-DB groups or to cluster proteomes into new ortholog groups. *Curr. Protoc. Bioinformatics* **35**, 6.12.11–6.12.19.

Ha, S.M., Kim, C.K., Roh, J., Byun, J.H., Yang, S.J., Choi, S.B., Chun, J., and Yong, D. 2019. Application of the whole genome-based bacterial identification system, TrueBac ID, using clinical isolates

that were not identified with three matrix-assisted laser desorption/ionization time-of-flight mass spectrometry (MALDI-TOF MS) systems. *Ann. Lab. Med.* **39**, 530–536.

Hiraishi, A., Ueda, Y., Ishihara, J., and Mori, T. 1996. Comparative lipoquinone analysis of influent sewage and activated sludge by high-performance liquid chromatography and photodiode array detection. *J. Gen. Appl. Microbiol.* **42**, 457–469.

Huan, Z., Yao, Y., Yu, J., Chen, H., Li, M., Yang, C., Zhao, B., Ni, Q., Zhang, M., Xie, M., *et al.* 2020. Differences in the gut microbiota between *Cercopithecinae* and *Colobinae* in captivity. *J. Microbiol.* **58**, 367–376.

Hwang, D.S., Lee, W.O., and Lee, J.S. 2013. Complete mitochondrial genome of the Korean bitterling *Acheilognathus koreensis* (Cypriniformes; Cyprinidae). *Mitochondrial DNA* **24**, 414–415.

Kim, D., Park, S., and Chun, J. 2021a. Introducing EzAAI: a pipeline for high throughput calculations of prokaryotic average amino acid identity. *J. Microbiol.* **59**, 476–480.

Kim, P.S., Shin, N.R., Lee, J.B., Kim, M.S., Whon, T.W., Hyun, D.W., Yun, J.H., Jung, M.J., Kim, J.Y., and Bae, J.W. 2021b. Host habitat is the major determinant of the gut microbiome of fish. *Microbiome* **9**, 166.

Kluge, A.G. and Farris, J.S. 1969. Quantitative phyletics and the evolution of anurans. *Syst. Zool.* **18**, 1–32.

Lane, D. 1991. 16S/23S rRNA sequencing. *In* Stackebrandt, E. and Goodfellow, M. (eds.), Nucleic Acid Techniques in Bacterial Systematics, pp. 115–175. John Wiley and Sons, New York, USA.

Lee, J.Y., Choi, J.S., Kim, J.K., Jang, Y.S., Lee, K.Y., and Kim, B.C. 2008. Ecological effects of Kumgang fat minnow (*Rhynchocypris kumgangensis*) on turbid water. *Korean J. Environ. Ecol.* **22**, 184–191.

Lee, S.Y., Kang, W., Kim, P.S., Kim, H.S., Sung, H., Shin, N.R., Whon, T.W., Yun, J.H., Lee, J.Y., Lee, J.Y., *et al.* 2019. *Undibacterium piscinae* sp. nov., isolated from Korean shiner intestine. *Int. J. Syst. Evol. Microbiol.* **69**, 3148–3154.

Lee, S.Y., Kang, W., Kim, P.S., Kim, H.S., Sung, H., Shin, N.R., Yun, J.H., Lee, J.Y., Lee, J.Y., Jung, M.J., *et al.* 2020. *Jeotgalibaca ciconiae* sp. nov., isolated from the faeces of an Oriental stork. *Int. J. Syst. Evol. Microbiol.* **70**, 3247–3254.

Lee, I., Kim, Y.O., Park, S.C., and Chun, J. 2016. OrthoANI: an improved algorithm and software for calculating average nucleotide identity. *Int. J. Syst. Evol. Microbiol.* **66**, 1100–1103.

Luo, C., Rodriguez-R, L.M., and Konstantinidis, K.T. 2014. MyTaxa: an advanced taxonomic classifier for genomic and metagenomic sequences. *Nucleic Acids Res.* **42**, e73.

Meier-Kolthoff, J.P., Auch, A.F., Klenk, H.P., and Göker, M. 2013. Genome sequence-based species delimitation with confidence intervals and improved distance functions. *BMC Bioinformatics* **14**, 60.

Minnikin, D., O'donnell, A., Goodfellow, M., Alderson, G., Athalye, M., Schaal, A., and Parlett, J. 1984. An integrated procedure for the extraction of bacterial isoprenoid quinones and polar lipids. *J. Microbiol. Methods* **2**, 233–241.

Na, S.I., Kim, Y.O., Yoon, S.H., Ha, S.M., Baek, I., and Chun, J. 2018. UBCG: up-to-date bacterial core gene set and pipeline for phylogenomic tree reconstruction. *J. Microbiol.* **56**, 281–285.

Price, M.N., Dehal, P.S., and Arkin, A.P. 2009. FastTree: computing large minimum evolution trees with profiles instead of a distance matrix. *Mol. Biol. Evol.* **26**, 1641–1650.

Saitou, N. and Nei, M. 1987. The neighbor-joining method: a new method for reconstructing phylogenetic trees. *Mol. Biol. Evol.* **4**, 406–425.

Sasser, M. 1990. Identification of bacteria by gas chromatography of cellular fatty acids. MIDI Technical Note 101. MIDI Inc., Newark, Delaware, USA.

Sohn, W.M., Na, B.K., Cho, S.H., and Ju, J.W. 2018. Infection status of *Isthmiophora hortensis* metacercariae in dark sleepers, *Odontobutis* species, from some water systems of the Republic of Korea. *Korean J. Parasitol.* **56**, 633–637.

Stackebrandt, E., Lang, E., Cousin, S., Päuker, O., Brambilla, E., Kroppenstedt, R., and Lünsdorf, H. 2007. *Deefgea rivuli* gen. nov., sp. nov., a member of the class *Betaproteobacteria*. *Int. J. Syst. Evol. Microbiol.* **57**, 639–645.

Thompson, J.D., Higgins, D.G., and Gibson, T.J. 1994. CLUSTAL W: improving the sensitivity of progressive multiple sequence alignment through sequence weighting, position-specific gap penalties and weight matrix choice. *Nucleic Acids Res.* **22**, 4673–4680.

Yang, H., Xiao, Y., Wang, J., Xiang, Y., Gong, Y., Wen, X., and Li, D. 2018. Core gut microbiota in Jinhua pigs and its correlation with strain, farm and weaning age. *J. Microbiol.* **56**, 346–355.

Yoon, S.H., Ha, S.M., Kwon, S., Lim, J., Kim, Y., Seo, H., and Chun, J. 2017. Introducing EzBioCloud: a taxonomically united database of 16S rRNA gene sequences and whole-genome assemblies. *Int. J. Syst. Evol. Microbiol.* **67**, 1613–1617.

Zhang, H., Yohe, T., Huang, L., Entwistle, S., Wu, P., Yang, Z., Busk, P.K., Xu, Y., and Yin, Y. 2018. dbCAN2: a meta server for automated carbohydrate-active enzyme annotation. *Nucleic Acids Res.* **46**, W95–W101.

Zhou, Y., Zhang, J., Zhang, D., Ma, W.-L., and Wang, X. 2021. Linking the gut microbiota to persistent symptoms in survivors of COVID-19 after discharge. *J. Microbiol.* **59**, 941–948.